A&A 482, L25–L28 (2008)
DOI: 10.1051/0004-6361:200809433

Astronomy & Astrophysics

Letter to the Editor

Transiting exoplanets from the CoRoT space mission

III. The spectroscopic transit of CoRoT-Exo-2b with SOPHIE and HARPS⋆

F. Bouchy[1], D. Queloz[2], M. Deleuil[3], B. Loeillet[1,3], A. P. Hatzes[4], S. Aigrain[5], R. Alonso[3], M. Auvergne[6], A. Baglin[6], P. Barge[3], W. Benz[7], P. Bordé[8], H. J. Deeg[9], R. De la Reza[10], R. Dvorak[11], A. Erikson[12], M. Fridlund[13], P. Gondoin[13], T. Guillot[14], G. Hébrard[1], L. Jorda[3], H. Lammer[15], A. Léger[8], A. Llebaria[3], P. Magain[16], M. Mayor[2], C. Moutou[3], M. Ollivier[8], M. Pätzold[17], F. Pepe[2], F. Pont[2], H. Rauer[12,19], D. Rouan[6], J. Schneider[18], A. H. M. J. Triaud[2], S. Udry[2], and G. Wuchterl[4]

(Affiliations can be found after the references)

Received 21 January 2008 / Accepted 6 March 2008

ABSTRACT

We report on the spectroscopic transit of the massive hot-Jupiter CoRoT-Exo-2b observed with the high-precision spectrographs SOPHIE and HARPS. By modeling the radial velocity anomaly occurring during the transit due to the Rossiter-McLaughlin (RM) effect, we determine the sky-projected angle between the stellar spin and the planetary orbital axis to be close to zero $\lambda = 7.2 \pm 4.5$ deg, and we secure the planetary nature of CoRoT-Exo-2b. We discuss the influence of the stellar activity on the RM modeling. Spectral analysis of the parent star from HARPS spectra are presented.

Key words. planetary systems – techniques: radial velocities

1. Introduction

Measurement of the spectroscopic signal during the transit of an exoplanet in front of its host star – known as the Rossiter-McLaughlin (RM) effect – provides an assessment the trajectory of the planet across the stellar disk and, more precisely, the sky-projected angle between the planetary orbital axis and the stellar rotation axis. This misalignment angle, denoted by λ, is a fundamental property of planetary systems that provides clues about the process of planet migration. Among the 30 transiting exoplanets known so far, λ has been reported for only 5 exoplanets (HD 209458b, Queloz et al. 2000; HD 189733b, Winn et al. 2006; HAT-P-2, Winn et al. 2007, Loeillet et al. 2008; HD 149026b, Wolf et al. 2007; and TrES-1, Narita et al. 2007). For all of these cases, λ is close to zero, as in the solar system, and the stellar rotation is prograde relative to the planet orbit. Such measurements should be extended to other transiting systems to understand whether this degree of alignment is typical.

The massive hot-Jupiter CoRoT-Exo-2b (Alonso et al. 2008) was revealed as planetary candidate by the CoRoT space mission (Baglin et al. 2003) and its planetary nature and mass was established thanks to ground-based facilities, including high-precision spectrographs SOPHIE (Bouchy et al. 2006) and HARPS (Mayor et al. 2003). This second CoRoT exoplanet is a 3.3 Jupiter-mass planet orbiting an active G7 dwarf star ($mv = 12.6$) every 1.743 days. We report here the measurements of the spectroscopic transit observed with both SOPHIE and HARPS spectrographs. These observations were made simultaneously with the space-based photometry with CoRoT. Such simultaneous monitoring is useful to assess anomalies in the transit parameters due to star spots or transient events.

Our data permits us to determine the sky-projected angle between the stellar spin and the planetary orbital axis, and it provids additional constraints on the orbital and physical parameters of the system. Furthermore, our data confirms and secures the planetary nature of the transiting body, excluding blending of an eclipsing binary with a third star as the cause of the observed shallow transits. We used HARPS spectra to perform the spectroscopic analysis of the parent star.

2. Observations

We performed high-precision radial velocity observations of CoRoT-Exo-2 ($mv = 12.6$) with the SOPHIE spectrograph, based on the 1.93-m OHP telescope (France), and the HARPS spectrograph, based on the 3.6-m ESO telescope (Chile). These two instruments are cross-dispersed, fiber-fed, echelle spectrographs dedicated to high-precision Doppler measurements based on the radial velocity techniques of simultaneous-thorium calibration. SOPHIE was used with its high efficiency mode (spectral resolution $R = 40\,000$). We reduced HARPS and SOPHIE data with the same pipeline based on the cross-correlation techniques (Baranne et al. 1996; Pepe et al. 2002). We observed CoRoT-Exo-2 with SOPHIE on 16 July 2007 and with HARPS on 1 September 2007. The exposure times were respectively 10 and 20 min on HARPS and SOPHIE corresponding to S/N per pixel at 550 nm of 16 and 25, respectively. We obtained the radial velocities by weighted cross-correlation with a numerical G2 mask constructed from the Sun spectrum atlas including up to 3645 lines. We eliminated the first 8 blue spectral orders

⋆ Observations made with SOPHIE spectrograph at Observatoire de Haute Provence, France (PNP.07A.MOUT) and HARPS spectrograph at ESO La Silla Observatory (079.C-0127(F)). The CoRoT space mission, launched on December 27th 2006, has been developed and is operated by CNES, with the contribution of Austria, Belgium, Brasil, ESA, Germany, and Spain.

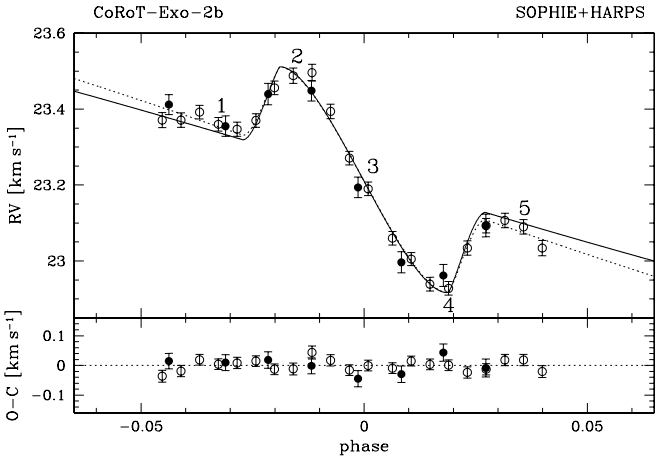

Fig. 1. Phase-folded radial velocity measurements of CoRoT-Exo-2 during the transit of the planet with SOPHIE (dark circle) and HARPS (open circle). The solid line corresponds to the Rossiter-McLaughlin model ajusted to these data assuming the semi-amplitude $K = 563$ m s^{-1} from Alonso et al. (2008). The dotted line corresponds to the Rossiter-McLaughlin model with K as free parameters.

containing only noise. Radial velocities are given in Table 1 and displayed in Fig. 1.

3. Rossiter-McLaughlin modeling

The RM effect corresponds to a distortion of the spectral lines observed during a planetary transit due to stellar rotation. The transiting body hides some of the velocity components that usually contribute to line broadening resulting in an Doppler-shift anomaly (see Otha et al. 2005; Giménez et al. 2006b; Gaudi & Winn 2007).

To model this RM effect, we used the analytical approach developed by Otha et al. (2005). The complete model has 12 parameters: the orbital period P; the mid-transit time T_c; the eccentricity e; the angle between the node and periastron ω; the RV semi-amplitude K; the velocity zero point V_0 (these first six are the standard orbital parameters); the radius ratio r_p/R_s; the orbital semi-major axis to stellar radius a/R_s (constrained by the transit duration); the sky-projected angle between the stellar spin axis and the planetary orbital axis λ; the sky-projected stellar rotational velocity $v \sin I$; the orbital inclination i; and the stellar limb-darkening coefficient ϵ. For our purpose, we started with the orbital parameters and photometric transit parameters as derived by Alonso et al. (2008). We fixed the linear limb-darkening coefficient $\epsilon = 0.78$, based on Claret (2004) tables for filter g' and for the stellar parameters derived in Sect. 4. Our free parameters are then λ and $v \sin I$. We introduced two additional parameters: the offset velocity of HARPS and SOPHIE, $\Delta_{\rm HARPS}$ and $\Delta_{\rm SOPHIE}$, which differ from V_0 due to the stellar activity. We determined the $v \sin I$ independently from SOPHIE cross-correlation functions (CCFs) to be 9.5 ± 1.0 km s^{-1} and from HARPS CCFs to be 10.7 ± 0.5 km s^{-1} with the calibration techniques described by Santos et al. (2002). However, we decided to leave it as free parameter in our fit.

The result of our fit, displayed in Fig. 1 and listed in Table 2, first shows that the stellar rotation is prograde relative to the planet orbit. During the first part of the transit the starlight is redshifted, indicating that the planet is in front of the approaching (blueshifted) half of the stellar disk. During the second part of transit, the sign is reversed as the planet moves to the receding (redshifted) half of the stellar disk. The sky-projected angle between the stellar spin axis and the planetary orbital axis λ is close to zero. The projected rotation velocity of the star $v \sin I$ determined by our RM fit (11.85 ± 0.5 km s^{-1}) seems slightly larger than our spectroscopic determination (2-σ greater). Previous studies by Winn et al. (2005) showed that the $v \sin I$ measured with Otha formulae was biased toward larger values by approximatively 10%. But, as already suggested by Loeillet et al. (2008), it may be due to the differential rotation of the star from equator to pole. Considering the exoplanet crosses the star near its equatorial plan, the fitted $v \sin I$ corresponds to the maximum value. Note that if we fix $v \sin I$ at the spectroscopic value, it does not change the value of the fitted λ angle.

We made the 2 epochs of RM observations at a minimum stellar flux (see Fig. 1 of Alonso et al. 2008), indicating that the stellar spots were at their maximum phase of visibility. Following the Saar & Donahue (1997) relation giving the expected RV jitter as a function of $v \sin I$ and spot filling factor, we found that CoRoT-Exo-2 is expected to present RV variations of up to 200 m s^{-1} peak-to-peak with a period of 4.5 days. The standard deviation of RV residuals (56 m s^{-1}) found by Alonso et al. (2008) is in agreement with this value. Such an activity-related RV variation should then change locally the apparent slope in the RV orbital curve. The maximum effect occurs at the maximum phase of stellar spot visibility, and should induce an apparent increase in the semi-amplitude K of up to 40 m s^{-1}. This explains why our fit in Fig. 1 is not perfect outside of the transit. If we increase K in our fit or leave it as a free parameter,

Table 1. Radial velocity measurements of CoRoT-Exo-2 obtained by HARPS and SOPHIE during the transit. BJD is the Barycentric Julian Date.

BJD −2 400 000	RV [km s^{-1}]	Uncertainty [km s^{-1}]
SOPHIE 2007-07-16		
54 298.4641	23.341	0.026
54 298.4862	23.285	0.027
54 298.5030	23.369	0.028
54 298.5198	23.378	0.027
54 298.5381	23.123	0.027
54 298.5550	22.926	0.028
54 298.5714	22.891	0.029
54 298.5879	23.023	0.030
HARPS 2007-09-01		
54 345.5225	23.371	0.020
54 345.5298	23.371	0.019
54 345.5371	23.392	0.018
54 345.5444	23.360	0.018
54 345.5517	23.347	0.019
54 345.5590	23.370	0.018
54 345.5663	23.456	0.018
54 345.5736	23.488	0.020
54 345.5809	23.496	0.022
54 345.5883	23.394	0.019
54 345.5956	23.271	0.018
54 345.6029	23.190	0.018
54 345.6124	23.060	0.018
54 345.6197	23.005	0.017
54 345.6270	22.939	0.018
54 345.6343	22.928	0.018
54 345.6417	23.034	0.019
54 345.6490	23.093	0.019
54 345.6563	23.107	0.019
54 345.6636	23.090	0.019
54 345.6709	23.034	0.020

Table 2. System parameters of CoRoT-Exo-2. The reduced χ^2 was computed assuming 24 degrees of freedom.

Fixed parameters from Alonso et al. (2008)	
P	1.7 429 964 days
T_c	54 237.53562
e	0.0
V_0	23.245 km s^{-1}
r_p/R_s	0.1667
a/R_s	6.70
i	87.84 deg
ϵ	0.78 (from Claret)
Adjusted parameters with K = 563 m s^{-1}	
$v \sin I$	11.85 ± 0.50 km s^{-1}
λ	7.2 ± 4.5 deg
Δ_{HARPS}	–21.5 ± 5 m s^{-1}
Δ_{SOPHIE}	+21.5 ± 12 m s^{-1}
reduced χ^2	1.43
Adjusted parameters with K as free parameter	
K	656 ± 27 m s^{-1}
$v \sin I$	11.25 ± 0.45 km s^{-1}
λ	5.0 ± 4.0 deg
Δ_{HARPS}	–25.0 ± 4.5 m s^{-1}
Δ_{SOPHIE}	+25.5 ± 11 m s^{-1}
reduced χ^2	1.01
Combined MCMC fit	
K	613 ± 14 m s^{-1}
$v \sin I$	$11.46^{+0.29}_{-0.44}$ km s^{-1}
λ	7.1 ± 5.0 deg
Δ_{HARPS}	–22.5 ± 4.5 m s^{-1}
Δ_{SOPHIE}	+23.5 ± 11 m s^{-1}
reduced χ^2	1.10

it significantly improves the fit and slightly decreases the value of $v \sin I$ and λ (see Table 2).

We also did a combined fitting of the photometry and the whole set of RV measurements. On each of the out-of-transit measurements, we inserted an additional error on the RV data to take the stellar activity into account. We chose this value as 56 m s^{-1}, corresponding to the standard deviation found by Alonso et al. (2008). This correction is justified since the action of activity on the points taken at random out-of-transit phases can be assumed as random for these points, while during transit we have sets of points with the same activity level throughout. The fitting was done using a Markov Chain Monte Carlo (MCMC) with a Metropolis-Hastings Algorithm for the decision process. We used the models of Giménez (2006a) and (2006b) for photometry and spectroscopic transits respectively. A quadratic law of limb darkening was used. For the photometry, we used the fitted parameters found by Alonso et al. (2008). For the spectroscopy parameters, we chose the V-band, from tables published by Claret (2000) for the stellar parameters derived in Sect. 4 ($u_+ = 0.748$, $u_- = 0.256$). The MCMC was performed over 20 000 accepted steps after 5000 steps of a burn-in period. The result of the combined fit is presented in Table 2, and is in full agreement with the other approachs.

The cross-correlation function (CCF) corresponds more or less to an average of all the spectral lines (see top of Fig. 2). In order to characterize the behavior of the spectral lines during the transit, we computed the difference between the HARPS CCFs corrected from the orbital velocity and a reference CCF taken out of the transit (more exactly an average of the 3 first exposures). This difference was computed at 5 epochs identified and labeled in Fig. 1 : (1) just before the ingress, (2) maximum of the RM effect, (3) mid-transit epoch, (4) minimum of the RM effect, (5) just after egress. These differences $\Delta CCF = CCF_{REF} - CCF_{\#}$

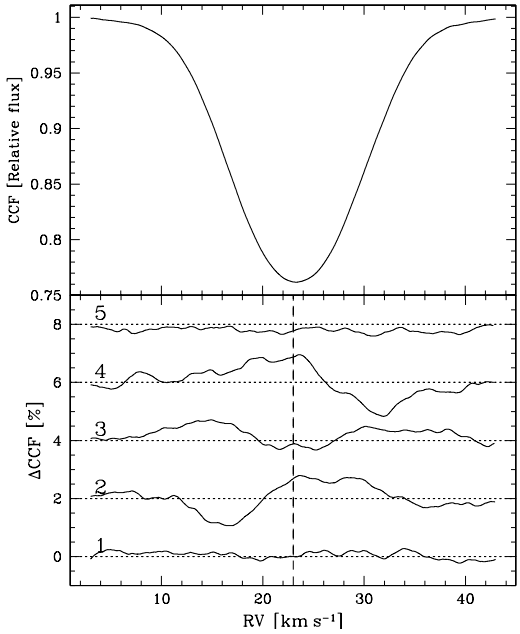

Fig. 2. (*Top*) Averaged cross-correlation function of CoRoT-Exo-2. (*Bottom*) Cross-correlation differences computed at 5 different epochs (see text) illustrating the behavior of the spectral lines during the transit.

are displayed in Fig. 2 and clearly show the spectroscopic anomaly shifting from the blue side (2) to the red side (4) of the CCF. During the transit, the depth or contrast of the CCFs is systematically larger, reflecting the renormalization effect of the CCF, which maintains a constant surface.

The observation of the spectroscopic transit of CoRoT-Exo-2b allows us to confirm definitively that the transiting candidate provided by CoRoT occurred at the central star (and not at a background star inside the CoRoT PSF). Furthermore, if we assume that the system is not diluted by an other star inside the HARPS or SOPHIE PSF, the RM anomaly reveals that the transiting body has a planetary size (from the RM anomaly amplitude) and planetary mass (from the RV slope outside the transit). In the case of an eclipsing binary whose light is diluted with a brighter third star, one should assume that the spectral lines of the fainter eclipsing binary move relative to the lines of the bright star and thus change the blended line-profiles. In such a configuration, one should consider not only the flux ratio but the $v \sin I$, velocity zero point, and spectral type of the two systems. In our present case, we did not find a configuration of a blended eclipsing binary that could simultaneously reproduce the RV anomaly and the photometric light curve. Furthermore, we computed RVs using different cross-correlation mask without significant changes in the shape and amplitude of the RM anomaly. We, thus, consider that the spectroscopic transit confirms and secures the planetary nature of the transiting body.

4. Spectroscopic analysis of CoRoT-Exo-2

We performed the spectroscopic analysis of the parent star using the HARPS spectra. We corrected individual spectra from the stellar velocity, rebinned to a constant wavelength step of 0.02 Å, and co-added spectral order per spectral order giving a S/N per pixel at 550 nm of about 80. We determined the effective temperature first from the analysis of the Hα line wings, providing a temperature of 5450 ± 120 K. In spite of the quite low S/N of the combined spectra, it appears that the star is at the border of the temperature domain in which the Hα line

wings are a good temperature indicator (from 5500 to 8500 K). We then checked this result with other methods. We performed synthetic spectra fitting using LTE MARCS atmosphere models (Gustafsson et al. 2005), which are well adapted for this range of temperature. We compared the synthetic spectra, previously convolved by the instrumental profile and a rotational profile with the $v \sin I$ value previously measured, to the observed one. The best-fit model yields a slightly higher temperature, but is still in agreement with the Hα estimate. Another analysis, using equivalent width measures of FeI and FeII lines, was also carried out and yields similar results. The adopted stellar parameters are $T_{\rm eff} = 5625 \pm 120$ K, $\log g = 4.3 \pm 0.2$ and [M/H] $= 0.0 \pm 0.1$, which correspond to a G7V type star with a solar metallicity. With these values, we derived the star's luminosity and mass with *StarEvolv* stellar evolution models (Siess 2006; Palacios, private communication). We combined these estimates of the star's mass to the $M_{\rm s}^{1/3}/R_{\rm s}$ value provided by the light curve analysis to derive the final star's mass and radius values in a consistent way between spectroscopic and photometric analyses. The method allows us to get rid of the large uncertainty that affects the estimate of the gravity and to take advantage of the excellent quality of the light curve. The method will be detailed in a forthcoming paper devoted to the fundamental parameters of the first CoRoT planet host stars, based on *UVES* spectra. The adopted stellar mass is $0.97 \pm 0.06\ M_{\odot}$ and the stellar radius is $0.90 \pm 0.02\ R_{\odot}$. Interestingly, the solar-like metallicity of the parent star and large radius of the planet is consistent with the trend that heavy element content in the planet and stellar metallicity are correlated (Guillot et al. 2006). According to stellar evolution models (Lebreton, private communication), the age of the star could be between 0.2 and 4 Gyr if the star is on the main sequence. However, the presence of the Li I absorption line and the strong emission line core in the CaII *H* and *K* lines, suggest that the star is still close the ZAMS and could be thus younger than 0.5 Gyr in full agreement with the observed stellar activity and the measured rotation period.

The knowledge of the main rotational period of CoRoT-Exo-2 determined from the light curve (4.54 days) and the spectroscopic $v \sin I$ determined from HARPS and SOPHIE CCFs (10.3 km s^{-1}) may be used to independently estimate the minimum radius of $R_s \sin I = 0.92\ R_{\odot}$ in very good agreement with our previous determination based on spectral classification. We note that this estimate, based on the well-determined stellar rotation thanks to the high-precision CoRoT light curve, does not depend on any spectral classification. On the other hand, if we assume the stellar radius from spectral analysis, we can deduce that $\sin I$ is close to 1, indicating a further constraint on the alignment of orbit and stellar spin.

5. Conclusions

In addition to the previous 5 transiting exoplanets where λ angle have been reported, CoRoT-Exo-2b presents a prograde orbit relative to the stellar rotation and an angle $\lambda = 7.2 \pm 4.5$ deg, close to zero. Our observations illustrate and demonstrate the capability of extending the reach of the RM technique to relatively-faint host stars ($mv \geq 12$) like the CoRoT targets even with a 2-m class telescope.

Acknowledgements. The authors wish to thank Xavier Bonfils and Gaspare Locurto for their precious help and support on HARPS observations. We are grateful for the OHP staff support at the 1.93-m telescope. The German CoRoT team (TLS and Univ. Cologne) acknowledges the support of DLR grants 50OW0603 and 50OW0204. F.B. acknowledges the support of PLS230371. H.J.D. acknowledges support by grants ESP2004-03855-C03-03 and ESP2007-65480-65480-C02-02 of the Spanish Education and Science ministry. The authors thank the referee for insightful comments and suggestions.

References

Alonso, R., Auvergne, M., Baglin, A., et al. 2008, A&A, 482, L21
Baglin, A., Auvergne, M., Boisnard, L., et al. 2006, in COSPAR, Plenary Meeting, 36th COSPAR Scientific Assembly, 36, 3749
Baranne, A., Queloz, D., Mayor, M., et al. 1994, A&AS, 119, 373
Bouchy, F., and the Sophie team 2006, in Tenth Anniversary of 51 Peg-b: Status of and prospects for hot Jupiter studies, ed. L. Arnold, F. Bouchy, & C. Moutou, 319
Claret, A. 2004, A&A, 428, 1001
Gaudi, B. S., & Winn, J. N. 2007, ApJ, 655, 550
Giménez, A. 2006a, A&A, 450, 1231
Giménez, A. 2006b, ApJ, 650, 408
Guillot, T., Santos, N. C., Pont, F., et al. 2006, A&A, 453, L21
Gustafsson, B., Asplund, M., Edvardsson, B., et al. 2005, IAU Symp. 228, ed. Francois & Primas (Cambridge University Press), 259
Loeillet, B., Shporer, A., Bouchy, F., et al. 2008, A&A, 481, 529
Mayor, M., Pepe, F., Queloz, D., et al. 2003, Messenger, 114, 20
Narita, N., Enya, K., Sato, B., et al. 2007, ApJ, 59, 763
Otha, Y., Taruya, A., & Suto, Y. 2005, ApJ, 622, 1118
Pepe, F., Mayor, M., Galland, F., et al. 2002, A&A, 388, 632
Queloz, D., Eggenberger, A., Mayor, M., et al. 2000, A&A, 359, L13
Saar, S. H., & Donahue, R. A. 1997, ApJ, 485, 319
Santos, N. C., Mayor, M., Naef, D., et al. 2002, A&A, 392, 215
Siess, L. 2006, A&A, 448, 717
Winn, J. N., Noyes, R. W., Holman, M. J., et al. 2005, ApJ, 631, 1215
Winn, J. N., Johnson, J. A., Marcy, G. W., et al. 2006, ApJ, 653, L69
Winn, J. N., Holman, M. J., Bakos, G. A., et al. 2007, ApJ, 665, L167
Wolf, A. S., Laughlin, G., Henry, G. W., et al. 2007, ApJ, 667, 549

[1] Institut d'Astrophysique de Paris, UMR7095 CNRS, Université Pierre & Marie Curie, 98bis Bd Arago, 75014 Paris, France
e-mail: bouchy@iap.fr
[2] Observatoire de Genève, Université de Genève, 51 Ch. des Maillettes, 1290 Sauverny, Switzerland
[3] Laboratoire d'Astrophysique de Marseille, CNRS UMR 6110, Traverse du Siphon, 13376 Marseille, France
[4] Thüringer Landessternwarte Tautenburg, Sternwarte 5, 07778 Tautenburg, Germany
[5] School of Physics, University of Exeter, Stocker Road, Exeter EX4 4QL, UK
[6] LESIA, CNRS UMR 8109, Observatoire de Paris, 5 place J. Janssen, 92195 Meudon Cedex, France
[7] Physikalisches Institut Universität Bern, Sidlerstrasse 5, 3012 Bern, Switzerland
[8] Institut d'Astrophysique Spatiale, Université Paris XI, 91405 Orsay, France
[9] Instituto de Astrofisica de Canarias, 38200 La Laguna, Tenerife, Spain
[10] Observatório Nacional, Rio de Janeiro, RJ, Brazil
[11] Institute for Astronomy, University of Vienna, Türkenschanzstr. 17, 1180 Vienna, Austria
[12] Institute of Planetary Research, DLR, Rutherfordstr. 2, 12489 Berlin, Germany
[13] Research and Scientific Support Department, European Space Agency, ESTEC, 2200 Noordwijk, The Netherlands
[14] Observatoire de la Côte d'Azur, Laboratoire Cassiopée, CNRS UMR 6202, BP 4229, 06304 Nice Cedex 4, France
[15] Space Research Institute, Austrian Academy of Sciences, Schmiedlstrasse 6, 8042 Graz, Austria
[16] Institut d'Astrophysique et de Géophysique, Université de Liège, Allée du 6 Août 17, Sart Tilman, Liège 1, Belgium
[17] Institute for Geophysics and Meteorology, Köln University, Albertus-Magnus-Platz, 50923 Cologne, Germany
[18] LUTH, Observatoire de Paris-Meudon, 5 place J. Janssen, 92195 Meudon Cedex, France
[19] Center for Astronomy and Astrophysics, TU Berlin, Hardenbergstr. 36, 10623 Berlin, Germany